JOURNAL OF SCIENCE TECHNOLOGY AND EDUCATION 14(1), MARCH, 2026
E-ISSN: 3093-0898, PRINT ISSN: 2277-0011; Journal homepage: www.atbufstejoste.com

Design and Simulation of ABUDrone: A Flight Control Platform for Security Surveillance

Dundu Lawan Haruna, Zaharuddeen Haruna, Hassan Maharazu, Abubakar Umar, Ibrahim Sufiyanu, Abdurrazaq Yahya
Faculty of Engineering
Ahmadu Bello University Zaria Nigeria

ABSTRACT
In recent years, Unmanned Aerial Vehicles (UAVs), particularly quadcopters, have gained significant attention from researchers worldwide due to their diverse applications in areas such as military surveillance, civilian monitoring, and disaster management. This project aims to design and simulate ABUDrone, a flight control platform tailored for security surveillance, addressing limitations in traditional surveillance methods, such as operator fatigue and delayed response times. A 3D physical model of ABUDrone was developed using Autodesk Tinkercad, designed as a lightweight quadcopter equipped with a high-precision camera for monitoring purposes. A Simulink model of the drone was created based on its mathematical dynamics, enabling effective control simulations. To enhance the project, a custom simulation environment, UAV3DSim, was designed using Simulink 3D Animation, modeling the Faculty of Engineering at Ahmadu Bello University (ABU), Zaria, including departments such as Computer, Electrical, Civil, and Mechanical Engineering, as well as the Kainji and Wolfson lecture theaters. Simulation results highlight the potential of the ABUDrone model and the UAV3DSim simulation platform as innovative tools for technology-driven security surveillance.

ARTICLE INFO
Article History
Received: October, 2025
Received in revised form: December, 2025
Accepted: January, 2026
Published online: March, 2026

KEYWORDS
Quadcopter, Security Surveillance, ABUDrone, Flight Control Platform, 3D model, Autodesk Tinkercad, High-Precision Camera, Simulink Model, Mathematical model, UAV3DSim Simulation Environment, Simulink 3D Animation,

INTRODUCTION

Unmanned aerial vehicles (UAVs) have received considerable amounts of attention from researchers and hobbyists worldwide in recent years due to their many potential applications. In particular, due to their excellent mobility and broad use in a range of applications, such as military operations, exploration, rescue missions, and surveillance, UAVs are broadly classified into two categories, which are fixed-wing and rotary-wing aircraft. Fixed-wing (FW) UAVs are simpler in structure, requiring less complex maintenance and repair, which contributes to their cost-effectiveness, longer operational times, and highspeed flight capabilities. Due to their abilities and capacity to carry a larger number of payloads over long distances with minimal power consumption, which make them ideal for various applications. However, fixed-wing UAVs are incapable of performing vertical take-off and landing, which limits their versatility compared to rotary-wing (RW) UAVs, which have the ability to perform Vertical take-off and land (VTOL) and hover, making them suitable for stationary applications such as inspections [1].

Rotary-wing UAVs, particularly quadrotors, have become increasingly popular due to their VTOL capabilities, agile maneuverability, and ease of development and maintenance. A quadrotor typically features an 'X' frame with four motors and propellers at each end, and its movements are controlled by varying the speed of these motors [1]. Despite being under actuated, making simultaneous control of all six degrees of freedom challenging, numerous control techniques have been developed to achieve

Corresponding author: Dundu Lawan Haruna
dundulawan90@gmail.com
Faculty of Engineering, Ahmadu Bello University Zaria, Nigeria.

JOURNAL OF SCIENCE TECHNOLOGY AND EDUCATION 14(1), MARCH, 2026
E-ISSN: 3093-0898, PRINT ISSN: 2277-0011; Journal homepage: www.atbufstejoste.com

autonomous flight, supported by advanced numerical models and simulation tools [2]. The UAV market, driven by these technological advancements, was valued at $18.14 billion USD and is projected to reach $52.30 billion USD by 2025. This growth reflects the expanding applications of UAVs in sectors such as media, fire services, power production, agriculture, delivery services, search and rescue, inspection, surveillance, and aerial photography [3].

Quadrotor Dynamics

Quadrotors are typically built in a plus configuration because of its ease of development and its popularity among various authors [4]. As shown in Fig. 1, 1 to 4 represent the angular velocities of motors 1 through 4, respectively. To achieve lift, motors 1 and 3 rotate clockwise, while motors 2 and 4 rotate counterclockwise. Adjusting the speed of each motor enables the UAV to move along specific axes. For instance, increasing the speed of all motors simultaneously results in vertical lift, as indicated by the arrows in Fig. 1(a). Increasing the speed of motor 2 while keeping the others constant induces pitch, shown in Fig. 1(b). Likewise, increasing motor 3's speed while maintaining the others at a constant speed produces roll, as illustrated in Fig. 1(c). Finally, increasing the angular velocity of motors 1 and 3 while reducing that of motors 2 and 4 generates a yawing motion.

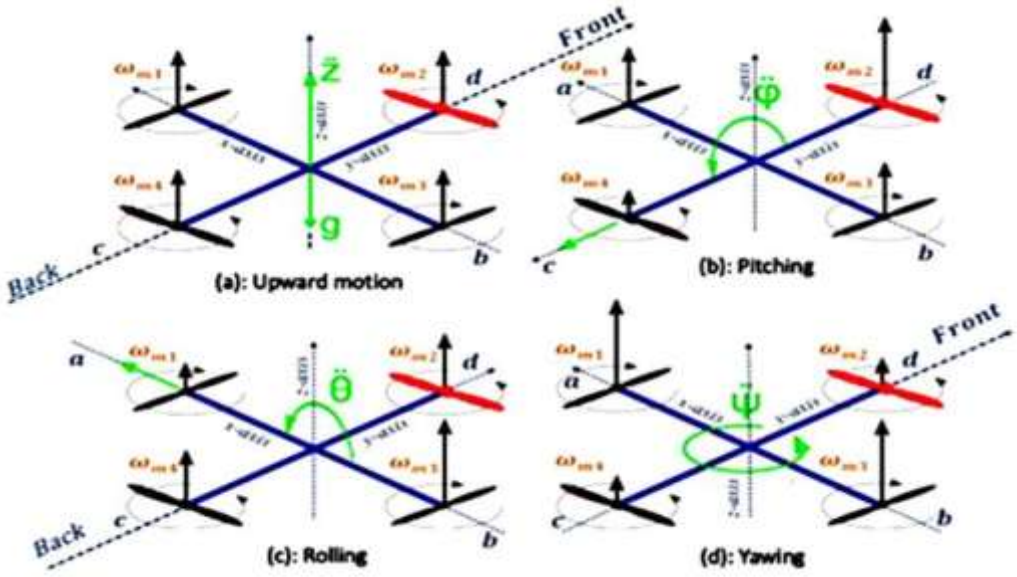

Fig. 1. Quadrotor Operation for; (a) Altitude, (b) Pitching, (c) Rolling, (d) yawing.

The dynamic description of the UAV is typically defined by twelve states x^T, as indicated by [4] and [5]. This can be mathematically represented in (1):

$$x^T = [x\ y\ z\ \dot{x}\ \dot{y}\ \dot{z}\ \phi\ \theta\ \psi\ \dot{\phi}\ \dot{\theta}\ \dot{\psi}] \quad (1)$$

where $\{x\ y\ z\ \dot{x}\ \dot{y}\ \dot{z}\}$ represents the respective positions and linear velocities, while $\{\phi\ \theta\ \psi\ \dot{\phi}\ \dot{\theta}\ \dot{\psi}\}$ signifies the respective angular positions and velocities of rolling, pitching and yawing.

.

Aerodynamic effects

Aerodynamic effects arise from propellers positioned parallel to the motor shafts, where thrust is generated as the angular velocity of the respective motors increases. This is mathematically described as [5,6,7]

$$T = Kw^2_i \quad (2)$$

where T represents the thrust generated for the corresponding angular velocity of the Brushless DC (BLDC)

Corresponding author: Dundu Lawan Haruna
dundulawan90@gmail.com
Faculty of Engineering, Ahmadu Bello University Zaria, Nigeria.

JOURNAL OF SCIENCE TECHNOLOGY AND EDUCATION 14(1), MARCH, 2026
E-ISSN: 3093-0898, PRINT ISSN: 2277-0011; Journal homepage: www.atbufstejoste.com

motor *i* is denoted by, and the constant K represents either the
thrust factor *b* or the drag factor *d*, depending on the desired
orientation of the quadrotor.

$$b = C_T \rho D^4 \quad (3)$$

$$d = C_p \rho D^5 \quad (4)$$

where CT and CP are the thrust and drag coefficients, ρ is the air density, and D is the propeller diameter. The parameters obtained from [8] represent the characteristics of
the propellers as shown in table 1.

Table I. Propeller characteristics

Parameter	*Symbol*	*Value*
Diameter	D	0.245m
Trust Coefficient	C_T	0.121
Power Coefficient	C_p	0.0495
Air density	P	1.255 Kg /m^3

Based on the values obtained from table 1, the thrust and drag factor are calculated as:

$$b = C_T \rho D^4 = 6.317 \times 10^{-4} \quad (5)$$

$$d = C_P \rho D^5 = 1.61 \times 10^{-4} \quad (6)$$

Motor conrol input

Since this research focuses on simulating a plusconfigured quadrotor, the thrust needed to achieve the desired motion is represented by the sum and difference of the forces from the four motors, as shown below:

$$\left.\begin{aligned} U_1 &= b(\Omega_1^2 + \Omega_2^2 + \Omega_3^2 + \Omega_4^2) \\ U_2 &= b(\Omega_4^2 - \Omega_2^2) \\ U_3 &= b(\Omega_3^2 - \Omega_1^2) \\ U_4 &= d(-\Omega_1^2 + \Omega_2^2 - \Omega_3^2 + \Omega_4^2) \end{aligned}\right\} \quad (7)$$

Where U_1 is the total thrust generated by the propellers, U_2, U_3, U_4 respectively represents the total thrust to achieve rolling, pitching and yawing, Ω_1, Ω_2, Ω_3, and Ω_4 represents the angular velocities of the motors.

The overall residual angular velocity (Ω_r) as the quadrotor rolls or pitches is defined as:

$$\Omega_+ = -\Omega + \Omega - \Omega_l + \Omega \quad (8)$$

Quadrotor equation of motion

The mathematical model of the quadrotor can be formulated using equations [9],[10],[11]and [12], which represent the translational and rotational accelerations. This model is derived from the Euler equations of motion and is expressed as follows:

$$\left.\begin{aligned} \ddot{x} &= \frac{U_1}{m}\left[cos\phi sin\theta cos\Psi - sin\Phi sin\Psi\right] \\ \ddot{y} &= \frac{U_1}{m}\left[cos\Phi sin\theta sin\Psi + sin\Phi cos\Psi\right] \\ \ddot{z} &= \frac{U_1}{m}\left[cos\phi cos\theta\right] - g \end{aligned}\right\} \quad (9)$$

$$\left.\begin{aligned} \ddot{\phi} &= \frac{1}{I_x}\left[\dot{\theta}\Psi(I_y - I_z) - J_r\dot{\theta}\Omega + lU_2\right] \\ \ddot{\theta} &= \frac{1}{I_y}\left[\dot{\theta}\Psi(I_z - I_x) - J_r\dot{\theta}\Omega + lU_3\right] \\ \ddot{\Psi} &= \frac{1}{I_g}\left[\dot{\theta}\Psi(I_x - I_y) + lU_4\right] \end{aligned}\right\} \quad (10)$$

Where, *m* represents the quadrotor's mass, *g* denotes gravitational acceleration, *l* indicates the distance from each rotor to the center of mass, and J_r stands for the moment of inertia of the motors. I_x, I_y and I_z respectively denotes the moments of inertia around the x, y, and z axes as indicated by [4] and [5].

The physical parameters used for studying the mathematical model of the quadrotor system are defined in Table II. as below.

TABLE II. Physical Parameters of Quadrotor

Parameter	**Symbol**	**Value**	**Units**
Thrust factor	b	6.317×10^{-4}	
Drag factor	d	1.61×10^{-4}	
Gravity force	g	9.81	m/s2
Inertia around x-axis	I_x	1.453×10^{-2}	Kgm^2

Corresponding author: Dundu Lawan Haruna
dundulawan90@gmail.com
Faculty of Engineering, Ahmadu Bello University Zaria, Nigeria.

JOURNAL OF SCIENCE TECHNOLOGY AND EDUCATION 14(1), MARCH, 2026
E-ISSN: 3093-0898, PRINT ISSN: 2277-0011; Journal homepage: www.atbufstejoste.com

Parameter	Symbol	Value	Units
Inertia around y-axis	I_y	1.453×10^{-2}	Kgm2
Inertia around z-axis	I_z	2.884×10^{-2}	Kgm^2
Motors moment of inertia	Jr	2.82×10^{-7}	
Length from rotor to center of mass	l	0.225	m
Quadrotor mass	m	1.888	Kg

Tinkercad

Tinkercad is a free, web-based 3D modeling tool launched in 2011, widely used for educational purposes and 3D printing. It simplifies constructive solid geometry by allowing users to create designs from basic shapes, which can be designated as "solid" or "hole" and combined into complex forms. Tinkercad supports importing STL, OBJ, and SVG files and can export models in STL or OBJ formats for 3D printing. Additional features include model exporting to Minecraft, Lego structure design, and a simulation lab for testing designs with components like motors and joints under gravity simulation as mention by [13] and [14].

Virtual reality modeling language

Virtual reality modeling language (VRMIL) Is a technology that provides the opportunity for creating virtual world with the ability to perform objects animation. It enables the navigation around the Virtual world, movement in D, interaction with objects, examining the virtual world using different viewpoints by users so that the world can appear as it is in the physical world as mention by [15].

Development of the Simulink Model of the UAV

The framework of the ABUDrone is shown in Fig. 2. It consists of the quadcopter's desired location defined by the x, y, and z coordinates as the input, a motor control algorithm based on the equations of motion (7), the ABUDrone model, which serves as the UAV plant based on the quadcopter dynamics equation (9) and (10), a 3D simulation environment developed using Simulink 3D Animation, and sensors for perception. This is shown in Fig. 2.

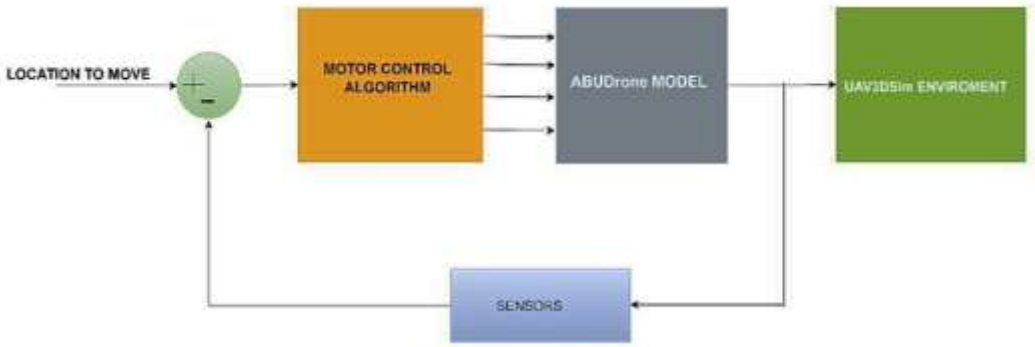

Fig. 2. Framework for ABUDrone

Development of the Simulink model of the UAV

The Simulink plant model of the drone is constructed based on Quadcopter dynamics (9) and (20). It features a subsystem that has x, y, z, and angles Φ, θ, Ψ as outputs, with inputs , , !, and as shown in Fig.3. This subsystem incorporates various components to represent different parameters according to their equations. The objective is to develop a comprehensive model encompassing all dynamic equations of the vehicle, which will be used to design a control system for the model.

Corresponding author: Dundu Lawan Haruna
dundulawan90@gmail.com
Faculty of Engineering, Ahmadu Bello University Zaria, Nigeria.

JOURNAL OF SCIENCE TECHNOLOGY AND EDUCATION 14(1), MARCH, 2026
E-ISSN: 3093-0898, PRINT ISSN: 2277-0011; Journal homepage: www.atbufstejoste.com

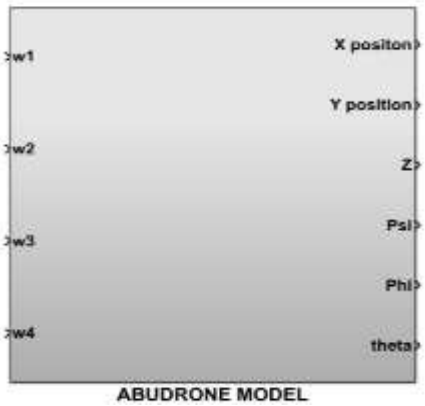

Fig. 3. Plant Model Subsystem

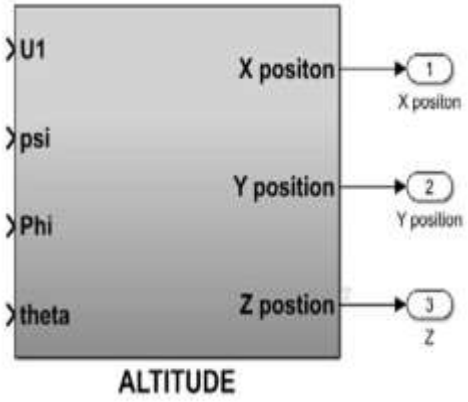

Fig. 5. Linear Acceleration Subsystem

Rotational Dynamics

This subsystem is based on (10) in which motors thrust is converted into angular position with the help of an integrator. It takes U_2, U_3, U_4 and omega from motors subsystem and outputs as angle psi, Phi and theta as shown in Fig.4. While U_1 is fed straight to the next subsystem, as U_1 is the total thrust of all motors in the Z direction.

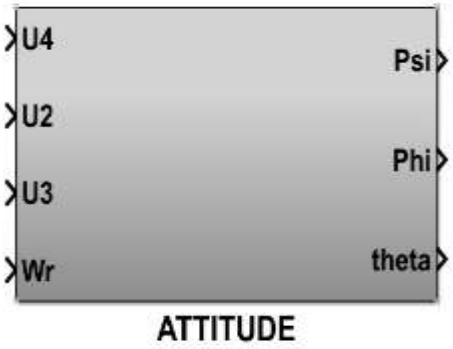

Fig. 4. Angular Position Subsystem

Translational Dynamics

Now the linear Position subsystem Fig.5 converts angles into the linear position in the inertial frame depending on navigation coordinate equation 3. To navigate the vehicle in the inertial coordinate frame, it takes the rotational angels Φ, θ, Ψ and U_1 as input and produce *X, Y* and *Z* as the position.

Motors control input

Motors control input shown in Fig.6 is a subsystem which depends on the moment equation for the specific orientation of the vehicle, since the main focus in this research is best on + configuration, (7) is used

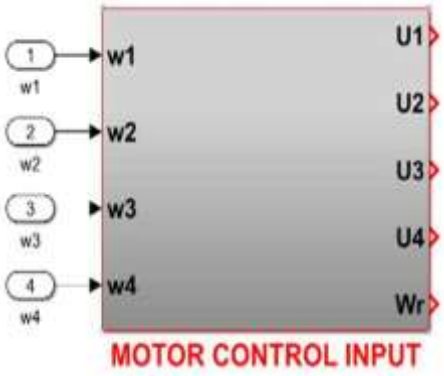

Fig. 6. Motors Control Input Subsystem

Development of the Abudrone

Thinker cad was used for the design of the UAV's 3D model. Fig.7 show the general 3D model of the UAV, which shows the integration of motors, propellers, and landing gear. These illustrations offer a detailed representation of the finalized design, highlighting its structural consistency and functional components. The 3D model consists of four-part, body frame, propellers, landing gear and payload.

Corresponding author: Dundu Lawan Haruna
dundulawan90@gmail.com
Faculty of Engineering, Ahmadu Bello University Zaria, Nigeria.

JOURNAL OF SCIENCE TECHNOLOGY AND EDUCATION 14(1), MARCH, 2026
E-ISSN: 3093-0898, PRINT ISSN: 2277-0011; Journal homepage: www.atbufstejoste.com

Fig. 7. ABUDrone Isometric View

Development of UAV3DSIM

The UAV3DSim environment was developed to simulate the plant model shown in Fig. 3, along with a 3D model of the ABUDrone, using Simulink 3D Animation. A VR Sink block enables interaction between the Simulink model in Fig. 3 and the 3D model in the virtual environment. The UAV3DSim environment, shown in Fig. 9, represents the Faculty of Engineering at Ahmadu Bello University, Zaria. It consists of blocks representing three departments and two lecture theaters, each serving as a potential target destination for the UAV. Departments are identified using D0 to D7 to denote coordinates. The UAV starts from a designated landing base. The virtual buildings, along with their dimensions and positions, are detailed in TABLE III.

Table III. Virtual Buildings in the Environment

Buildi ngs	Description	Dimension	Position	Door
D0	Computer	[400 200 100]	[200 100 -300]	[60 30 200]
D1	Telcom	[400 200 100]	[200 100 -300]	[35 30 200]
D2	Electrical	[600 200 100]	[80 100 -100]	[0 0 -65]
D3	Mechanical	[100 200 400]	[400 100 200]	[430 30180]
D4	Civil	[100 200 500]	[-450 100 50]	[-350 30 10]
D5	High voltage	[150 200 150]	[-150 100 -280]	[-150 0 -15]
D6	Wolfson	[500 80 140]	[0 35 350]	[-10 10 400]

Location of other objects in the environment like UAV and street light are presented in TABLE IV

Table IV. Virtual Objects in the Environment

Object	Dimensions	Position
UAV	[20 20 20]	[-350 0.2 350]
Road1	[2000 0.5 150]	[0 0 -550]
Street light	[50 300 50]	[920 0 550]
Round about	Radius = 150	[900 0 -500]

To clearly differentiate the objects in the environment, spot light and viewpoints are added with their parameters presented in TABLE V.

Table V. Spot Light and Viewpoints

Object	Position	Orientation	dime
Spot Light	[2500 3500 4500]	[0 0 -1]	R=100
Top View	[100 200 -35]	[-1 0 0]	900
Side View	[90 80 235]	[0 0 1]	00

The final UAV3DSim environment is shown in Fig. 8 (side view) and Fig. 9 (top view), respectively.

Fig. 8. Side View of UAV3DSim Environment

Corresponding author: Dundu Lawan Haruna
dundulawan90@gmail.com
Faculty of Engineering, Ahmadu Bello University Zaria, Nigeria.

JOURNAL OF SCIENCE TECHNOLOGY AND EDUCATION 14(1), MARCH, 2026
E-ISSN: 3093-0898, PRINT ISSN: 2277-0011; Journal homepage: www.atbufstejoste.com

Fig. 9. Top View of UAV3DSim Environment

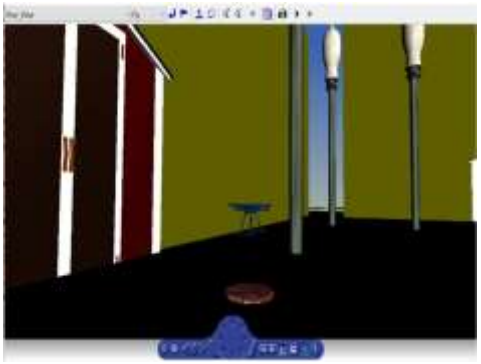

Fig. 10. Side Camera Attached to the UAV

The UAV3DSim environment was integrated to the Simulink model developed for UAV navigation with go to capability through the VR Sink block. The VR Sink block enables access to the translation and rotation of the vehicle in the virtual environment from the Simulink environment. A camera was attached to the vehicle, which enables the visualization of the side of the vehicle as it moves from start position to any target destination. This is shown in Fig. 10.

Fig.10.shows the developed 3D simulation environment integrated with the Simulink model of the UAV. This integration allows for real-time interaction between the UAV's dynamic model and its virtual environment, enabling comprehensive testing and visualization of the UAV's movements and control responses. Through this setup, users can observe the UAV's behavior in the simulated environment, which closely mimics real-world conditions, supporting effective analysis and refinement of control strategies.

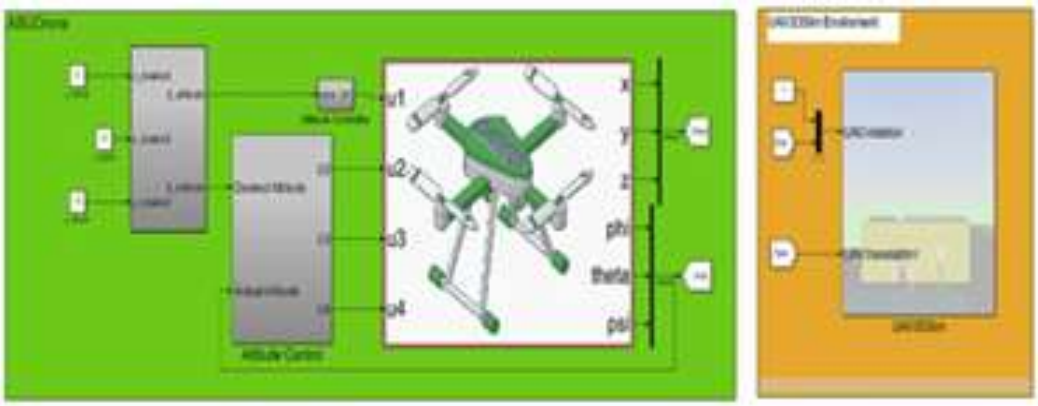

Fig. 11. Developed 3D Simulation Environment Integrated with Simulink Model of the UAV

Simulation Results and Analysis

In this section, the aim is to simulate the ABUDrone in the UAV3DSim environment. Simulink was utilized for the simulation of the ABUDrone, while the UAV 3D environment was employed for visualizing the overall model, as shown in Fig. 11.

The quadcopter model was verified by applying motor speed inputs and observing the system's response. The simulation utilized predefined motor thrust values to assess the

Corresponding author: Dundu Lawan Haruna
dundulawan90@gmail.com
Faculty of Engineering, Ahmadu Bello University Zaria, Nigeria.

JOURNAL OF SCIENCE TECHNOLOGY AND EDUCATION 14(1), MARCH, 2026
E-ISSN: 3093-0898, PRINT ISSN: 2277-0011; Journal homepage: www.atbufstejoste.com

UAV's takeoff and navigation capabilities. Real-world constraints were incorporated into the model, including a zero lower limit for altitude to prevent the UAV from descending below the Earth's surface.

Upward Movement

To evaluate the quadcopter's takeoff capability, all motors were set to generate a thrust of 5 N (88.9 RPS) for 2 seconds. This setup was intended to achieve upward movement. The results, shown in Fig.12, Fig .13 and Fig.14 demonstrate that the quadcopter successfully increased its altitude while maintaining stable roll, pitch, and yaw angles. This confirms that the model's thrust requirements are adequate for achieving lift-off.

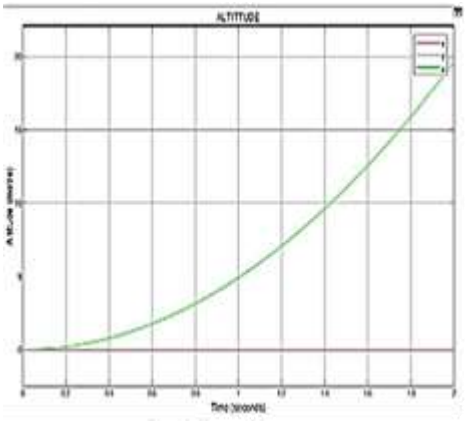

Fig. 12. Upward Movement

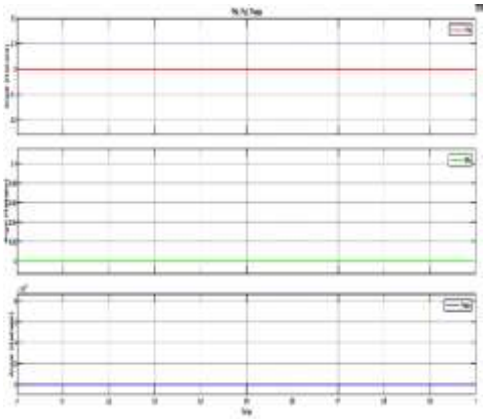

Fig. 13. Rotation Angles

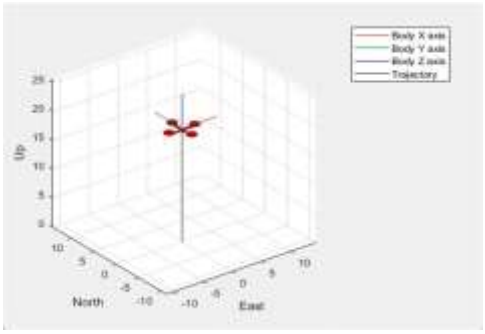

Fig. 14. Upward Movement in 3D Space

Pith and Lateral Movement

For the assessment of pitch and lateral movements, motor 1 and motor 2 were configured to produce 5 N of thrust each, while motors 3 and 4 were set to 2 N. Fig.15 and Fig.16 illustrate the resulting pitch and lateral movements. The simulations confirm that the quadcopter can achieve the desired pitch and lateral adjustments, validating the model's ability to handle these maneuvers effectively.

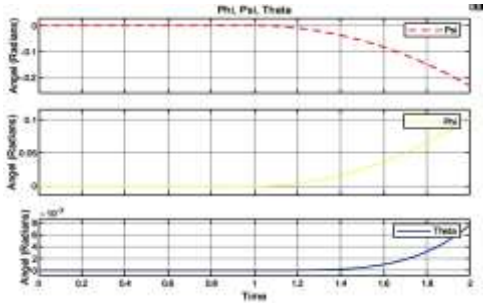

Fig. 15. Pitch and Lateral Movement in 3D Space

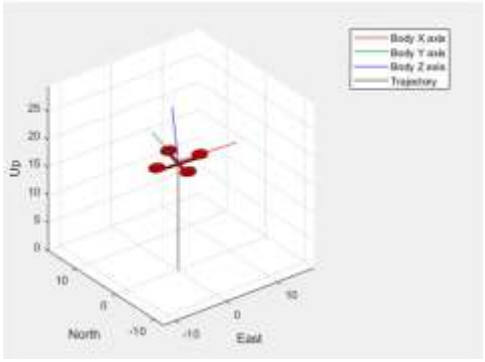

Fig. 16. Pitch and Lateral Movement

Corresponding author: Dundu Lawan Haruna
dundulawan90@gmail.com
Faculty of Engineering, Ahmadu Bello University Zaria, Nigeria.

JOURNAL OF SCIENCE TECHNOLOGY AND EDUCATION 14(1), MARCH, 2026
E-ISSN: 3093-0898, PRINT ISSN: 2277-0011; Journal homepage: www.atbufstejoste.com

Roll and Lateral Movement

To evaluate roll and lateral movement apabilities, motor 1 and motor 4 were set to 2 N of thrust,while motor 2 and motor 3 were set to 5 N. Fig.17 and Fig.18 display the outcomes, demonstrating the quadcopter's performance in achieving roll and lateral adjustments. The results indicate that the model accurately simulates roll dynamics and lateral movement under the given thrust settings.

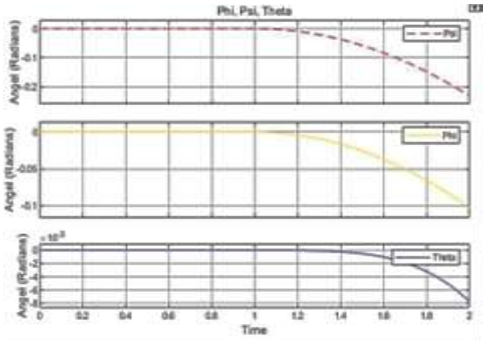

Fig. 17. Roll and Lateral Movement

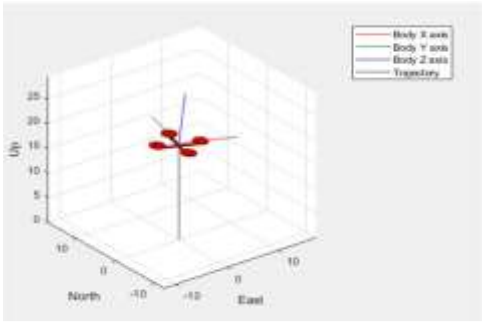

Fig. 18. Roll and Lateral Movement in 3D Space

3D Simulation Environment Using UAV3DSim and Simulink 3D Animation

The 3D simulation environment, UAV3DSim, was utilized to visualize the quadcopter's behavior in various scenarios using Simulink 3D Animation. The results obtained from the simulation are presented through three different views: top view, side view and a camera view attached to the vehicle. The simulation model referenced in Fig.10 was used for these visualizations.

Side View of the Simulation Environment

Fig. 19 shows the side view of the UAV3Dsim environment. In this view, the quadcopter is positioned at its starting location with the target destination clearly marked. This view provides a clear perspective of the UAV's initial and target positions, allowing for an assessment of the trajectory and movement.

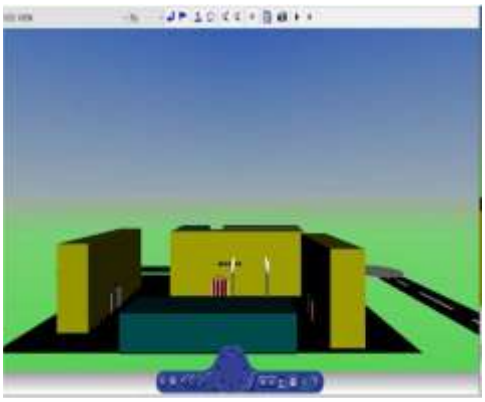

Fig. 19 Side View of the Simulation Environment

Camera View Attached to the Vehicle

Fig. 20 depicts the side view from the camera attached to the UAV. This view captures the `perspective of the quadcopter as it navigates through the simulation environment. The camera view provides additional insight into the UAV's real-time navigation and its interaction with the environment.

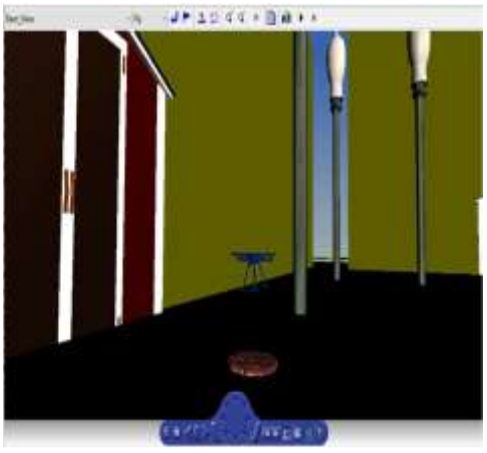

Fig. 20. Camera View Attached to the Vehicle

Corresponding author: Dundu Lawan Haruna
dundulawan90@gmail.com
Faculty of Engineering, Ahmadu Bello University Zaria, Nigeria.

JOURNAL OF SCIENCE TECHNOLOGY AND EDUCATION 14(1), MARCH, 2026
E-ISSN: 3093-0898, PRINT ISSN: 2277-0011; Journal homepage: www.atbufstejoste.com

Top View of the Simulation Environment

Fig.21 shows the top view of the UAV3DSim environment. This view captures the aerial perspective of the quadcopter's movement towards the target destination. The top view provides a comprehensive overview of the UAV's path and positioning relative to the target.

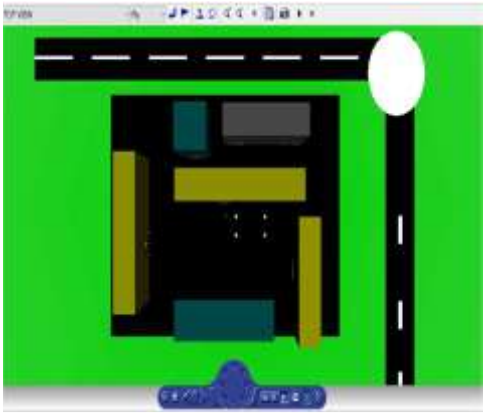

Fig. 21. Top View of the Simulation Environment

CONCLUSION

This research successfully developed and simulated a flight control platform for the ABUDrone using MATLAB/Simulink and Tinkercad. By implementing a detailed dynamic model of the UAV and constructing a realistic virtual environment, the simulation demonstrated the potential of UAV technology to be applied in various operations within Ahmadu Bello University (ABU), Zaria. The integration of control inputs such as roll, pitch, yaw, and throttle showcased the platform's effectiveness in achieving stable flight and accurate navigation. The creation of a 3D model of the ABUDrone and its integration with a virtual representation of ABU's Faculty of Engineering further emphasized the practical applications of UAVs in academia. Overall, the project achieved its objective of demonstrating the capabilities of UAV technology through simulation and design. The results demonstrate the potential for implementing security surveillance in university settings using UAV technology.

REFERENCES

[1] [10] M. Mahbub et al., "A review of UAVs topologies and control techniques," *IEEE Conference on Unmanned Systems*, 2021. [Online]. Available: https://ieeexplore.ieee.org/document/9465186.

[2] A. Idris et al., "A survey of vertical takeoff and landing (VTOL) and hovering applications in UAVs," International Journal of Advanced Research in Engineering and Technology, vol. 12, no. 2, pp. 23–34, 2021. [Online]. Available: https://ijaret.com.

[3] I. Usman, "The UAV market growth report: Valuation and applications across industries," Drone Industry Insights, 2020. [Online]. Available: https://droneii.com/uav-market-growth-report.

[4] X. Zhang, X. Li, K. Wang and Y. Lu, "A survey of modelling and identification of quadrotor robot," *In Abstract and Applied Analysis, Hindawi,* 2014.

[5] H. B. Mitchell, J. A. S. Vargas, and M. N. Rojas, "Aerodynamics of Quadrotor Drones," *Journal of Aircraft Engineering*, vol. 92, no. 5, pp. 207-216, 2020.

[6] M. D. M. Zia and A. R. Khan, "Performance Analysis of Propellers in Quadrotor Drones," *International Journal of Aerospace Engineering*, vol. 2021, Article ID 6821934, 2021.

[7] R. C. M. Demarco and S. T. Oliveira, "Mathematical Modeling of Quadrotor Thrust Dynamics," *IEEE Transactions on Aerospace and Electronic Systems*, vol. 58, no. 1, pp. 234-245, 2022.

[8] S. K. S. Mandal, A. B. Ghosh, and S. S. Jha, "Performance Analysis of UAV Propellers: A Review," *International Journal of Aerospace Engineering*, vol. 2021, Article ID 7885073, 2021. DOI: 10.1155/2021/7885073.

[9] A. Salih, M. Moghavvemi, H. Mohamed, and K. Gaeid, "Flight PID controller design for a UAV quadrotor," *Scientific Research and Essays*, vol. 5, no. 23, pp. 3660-3667, 2010.

[10] [6] M. Efe, "Robust low altitude behavior control of a quadrotor rotorcraft through sliding modes," *Mediterranean Conference*

Corresponding author: Dundu Lawan Haruna
dundulawan90@gmail.com
Faculty of Engineering, Ahmadu Bello University Zaria, Nigeria.

on Control and Automation, pp. 1-6, IEEE, 2007.

[11] [7] E. Zheng, J. Xiong, and J. Luo, "Second order sliding mode control for a quadrotor UAV," *ISA Transactions*, vol. 53, no. 4, pp. 1350-1356, 2014.

[12] [8] A. Rusli, M. Aras, M. Aripin, M. Kamarudin, M. Azmi, M. Kasno, A. Khamis, and Z. Rizman, "Modeling of unmanned aerial vehicle (UAV) for altitude control using system identification technique," *Journal of Fundamental and Applied Sciences*, vol. 10, pp. 936-950, 2018.

[13] Autodesk, "Tinkercad: Easy-to-use 3D CAD design tool," Autodesk, Accessed: Nov. 13, 2023. [Online]. Available: https://www.autodesk.com/products/tinkercad/overview.

[14] Wikipedia, "Tinkercad," *Wikipedia*, Accessed: Nov. 13, 2023. [Online]. Available:

[15] D. R. Deering, "High-Performance Graphics for the World Wide Web," *Computer Graphics*, vol. 30, no. 2, pp. 45-56, 1996. [Online]. Available: https://www.w3.org/MarkUp/VRML/.

Corresponding author: Dundu Lawan Haruna
dundulawan90@gmail.com
Faculty of Engineering, Ahmadu Bello University Zaria, Nigeria.